Journal of Asian Earth Sciences 35 (2009) 45–55

Contents lists available at ScienceDirect

Journal of Asian Earth Sciences

journal homepage: www.elsevier.com/locate/jaes

Zircon Lu–Hf isotopic compositions of metaluminous and peralkaline A-type granitic plutons of the Emeishan large igneous province (SW China): Constraints on the mantle source

J. Gregory Shellnutt [a,*], Christina Yan Wang [b], Mei-Fu Zhou [c], Yueheng Yang [d]

[a] Academia Sinica, Institute of Earth Science, 128 Academia Road Sec. 2, Nankang, Taipei 11529, Taiwan
[b] Guangzhou Institute of Geochemistry, Chinese Academy of Sciences, Guangzhou 510640, China
[c] Department of Earth Sciences, The University of Hong Kong, Hong Kong SAR, China
[d] State Key Laboratory of Lithospheric Evolution, Institute of Geology and Geophysics, Chinese Academy of Sciences, Beijing 100029, China

ARTICLE INFO

Article history:
Received 22 May 2008
Received in revised form 30 November 2008
Accepted 30 December 2008

Keywords:
Zircon Lu–Hf isotope
A-type granite
Peralkaline
Metaluminous
Panxi region
SW China

ABSTRACT

Permian A-type granitoids of the Emeishan large igneous province (ELIP) in the Panxi region, SW China, are predominantly peralkaline and metaluminous in composition. In situ zircon Hf isotopic compositions along with whole rock trace element and Nd isotopic data are used to examine the probable source characteristics of these A-type granitic plutons. Zircons from the Baima and Taihe peralkaline plutons have weighted average $\varepsilon Hf_{(T)}$ values of +8.7 ± 0.4 and +9.2 ± 1.0, whereas the Woshui and Huangcao metaluminous plutons have differing $\varepsilon Hf_{(T)}$ values (+8.6 ± 0.2 and +5.8 ± 0.3, respectively). Previous studies have suggested that the plutons were derived by differentiation (e.g. fractionation or partial melting) of mafic magmas from an enriched mantle source similar to oceanic island basalt with little or no contribution from the crust ($\varepsilon Nd_{(T)}$ = +1.3 to +3.2, Zr/Nb = 0.9–14.4, Rb/Nb = 0.1–8.4 and Th/Ta = <4.0). Therefore, we interpret the Hf isotopic data of the Baima, Taihe, Woshui and Huangcao plutons to be indicative of the Emeishan mantle plume. The similar zircon $\varepsilon Hf_{(T)}$ values of the Woshui and Baima plutons indicates that spatially and temporally associated peralkaline and metaluminous A-type granitic rocks can originate from the same mantle source without crustal assimilation.

1. Introduction

The petrogenesis of A-type granitoids is controversial (Collins et al., 1982; Eby, 1992; Frost and Frost, 1997; Goodge and Vervoort, 2006; Bonin, 2007). Peralkaline granitoids are almost synonymous with A-type characteristics, whereas metaluminous and peraluminous are less likely to be so (King et al., 1997). Temporally and spatially associated peralkaline and metaluminous A-type granitic plutons are common within the continental crust although the individual rock types usually have mutually exclusive petrogenetic histories (Poitrasson et al., 1995; Frost and Frost, 1997; Shellnutt and Zhou, 2007). Spatial, temporal and geochemical evidence suggest that some peralkaline granitic rocks can form by fractionation of mantle-derived mafic parental rocks (Bonin, 2007; Shellnutt et al., in press). However, peralkaline rocks may have chemical characteristics (e.g. negative Nb anomaly and elevated $^{87}Sr/^{86}Sr$) indicative of metasomatized lithospheric mantle or continental crust (Turner et al., 1992; Kemp et al., 2005; Yang et al., 2006). On the other hand, metaluminous granitic rocks are commonly thought to be derived from a mixed (crust + mantle) source (Poitrasson et al., 1995; Schmitt et al., 2000; Kemp et al., 2005; Bonin, 2007).

The Late (260 Ma) Permian Emeishan large igneous province (ELIP) in SW China contains numerous A-type granitic plutons associated with layered mafic intrusions which host magmatic Fe–Ti–V oxide deposits (Zhou et al., 2002; Shellnutt and Zhou, 2007; Zhong et al., 2007). The plutons in the ELIP mainly occur in the Panxi region and are mostly peralkaline and metaluminous in composition. The peralkaline plutons contain hypersolvus feldspar, Fe–Na-rich pyroxene and amphibole, have high Ga/Al ratios and high field strength elements and negative Eu/Eu^* values, all of which are characteristic of A-type granitic rocks (Loiselle and Wones, 1979; Whalen et al., 1987; Bonin, 2007). The metaluminous plutons are similar to the peralkaline plutons in having hypersolvus feldspar and high Ga/Al ratios, but they are poor in Th, U, Zr and Hf and have positive Eu/Eu^* values. Previous Sr–Nd isotopic studies of the ELIP granitoids have suggested that the two types of plutons originated from the same mantle source (Shellnutt and Zhou, 2007, 2008). However, granitic rocks, especially peralkaline rocks, may be susceptible to isotopic disturbance and thus the Rb–Sr and Sm–Nd isotopic system may not be well suited for characterizing their sources (Vervoort et al., 1996;

* Corresponding author.
E-mail addresses: jgshelln@earth.edu.tw, gshellnutt@hotmail.com (J. Gregory Shellnutt).

1367-9120/$ - see front matter © 2009 Elsevier Ltd. All rights reserved.
doi:10.1016/j.jseaes.2008.12.003

Nowell et al., 1998; Poitrasson et al., 1998; Kempton et al., 2000). In contrast, the zircon Lu–Hf isotopic system is resistant to element mobility and preserves the original $^{176}Hf/^{177}Hf$ ratio of the parental melt and is therefore very useful for constraining the composition of the magma source from which the zircon crystallized (Salters, 1996; Vervoort et al., 1996; Poitrasson et al., 1998; Salters and White, 1998; Schmitt et al., 2000; Chauvel and Blichert-Toft, 2001; Kinny and Maas, 2003; Kemp et al., 2005, 2007).

Previous zircon Hf isotopic studies of contemporaneous peralkaline and metaluminous granitic plutons indicate that they originate from depleted mantle and mixed (e.g. crust + depleted mantle) sources, respectively (Wu et al., 2002; Kemp et al., 2005; Xu et al., 2008). In this study, we present zircon Hf isotope data for peralkaline and metaluminous A-type granitic plutons (i.e. Baima, Taihe, Woshui and Huangcao) of the ELIP from the Panxi region, SW China. This new dataset, together with available whole rock trace elemental and Nd isotopic data, enable us to better constrain and characterize their source composition.

2. Panxi A-type granitoids of the ELIP

The ELIP is located in a region covering an area of $\sim 0.3 \times 10^6$ km^2 in the western part of the Yangtze Block, eastern part of the Tibetan Plateau (i.e. Songpan-Ganze terrane) and northern Vietnam, and has been modified by Mesozoic and Cenozoic faulting associated with the eastward extrusion of the Tibetan Plateau during the Indo-Eurasian collision (Fig. 1). The ELIP consists of high- and low-Ti flood basalts, felsic plutons and mafic–ultramafic intrusions which host either Ni–Cu–(PGE) sulfide deposits or giant Fe–Ti–V oxide deposits (Ali et al., 2005; Zhou et al., 2008). The ELIP is geologically and geochronologically constrained to the Late Permian with radiometric ages ranging from ~260 to ~251 Ma (Shellnutt et al., 2008). Previous studies of the flood basalts suggest that the ELIP was mantle plume-derived (Chung and Jahn, 1995; Chung et al., 1998; Xu et al., 2001).

A-type granitic plutons of the ELIP primarily occur in the Panxi region, SW China (Shellnutt and Zhou, 2007; Zhong et al., 2007) (Fig. 1). They are distributed at intervals of tens of kilometers along a narrow belt ~50 km wide and ~200 km long. The regional distribution trend of the plutons changes from northeast-southwest to north-south near the town of Miyi at the central part of the Panxi region (Fig. 1). The plutons are of peralkaline, peraluminous and metaluminous compositions and are spatially and temporally associated with Fe–Ti oxide ore-bearing layered gabbroic intrusions (Shellnutt and Zhou, 2007; Zhong et al., 2007). The Baima and Taihe peralkaline plutons are spatially and genetically associated with Fe–Ti oxide bearing layered gabbroic intrusions and were emplaced at ~260 Ma (Xu et al., 2008; Shellnutt et al., in press). These two peralkaline plutons are located ~100 km apart in the central and northern part of the Panxi region (Fig. 1). The Baima peralkaline pluton and layered gabbroic intrusion are comagmatic and cogenetic and form the Baima igneous complex (BIC) (Shellnutt et al., in press). Surrounding the BIC are the Woshui and Huangcao metaluminous plutons. The ~260 Ma Woshui pluton is to the east of the BIC and intrudes the lower part of the layered gabbroic unit (Fig. 1), indicating that the Woshui pluton is slightly younger than the BIC (Shellnutt and Zhou, 2007). The fayalite- and quartz-bear-

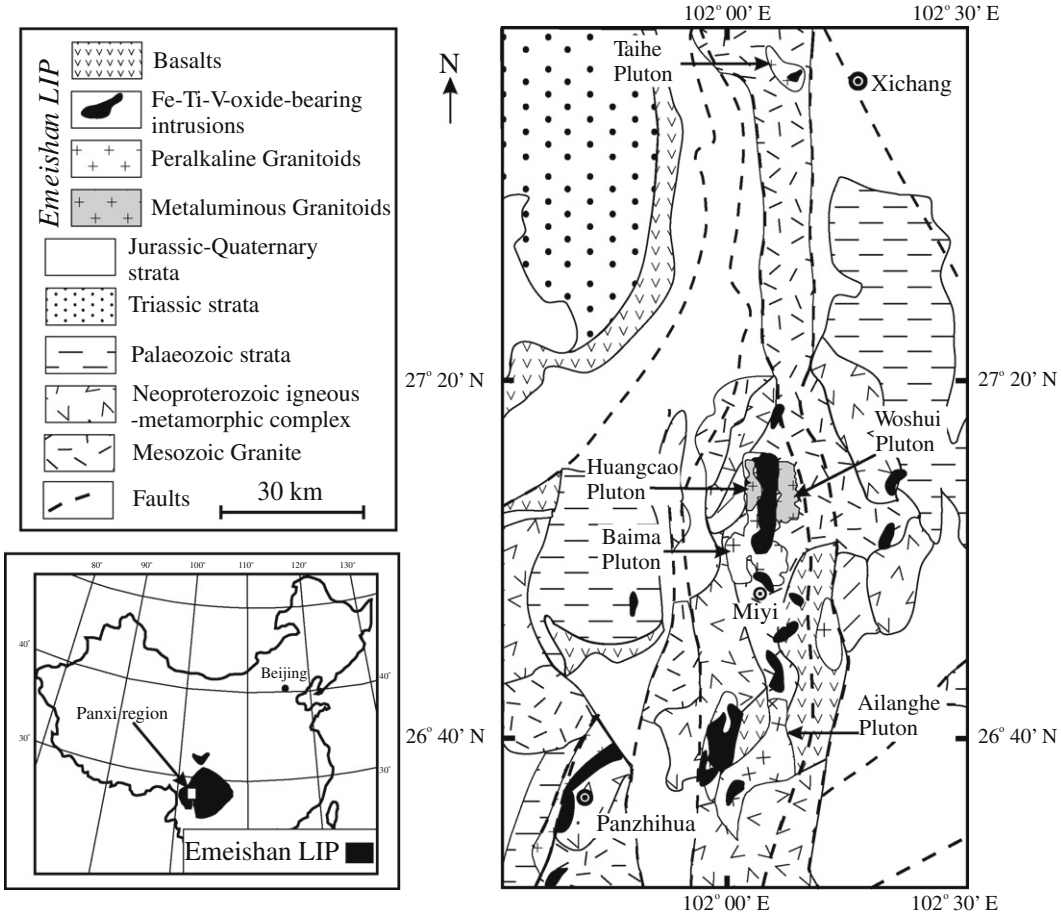

Fig. 1. Simplified geological map of the Panxi region showing the locations of the Baima, Huangcao, Woshui, Taihe and Ailanghe plutons.

ing Huangcao pluton intrudes the western portion of the BIC and is ~252 Ma (Fig. 1) (Shellnutt and Zhou, 2008).

3. Analytical method and results

Zircons were separated from five samples of the Woshui pluton, three samples from the Huangcao pluton and one sample each from the Taihe and Baima plutons. The zircons are typically fragmented and show diffuse and metamict oscillatory zonation (Griffin et al., 2006). Lu–Hf isotope compositions of zircon grains were analyzed in situ using a Geolas-193 laser-ablation microprobe, attached to a Neptune multi-collector ICP-MS, at the Institute of Geology and Geophysics, Chinese Academy of Sciences, Beijing. More detail experimental conditions and data collection were described by Wu et al. (2006). The results are listed in Table 1. Ablation time for each analysis is about 30 s for 200 cycles of each measurement, with a 10 Hz repetition rate and 100 mJ/pulse laser power. During the analyses, a stationary spot was used with a beam diameter of about 63 μm. Isobaric interference of ^{176}Lu on ^{176}Hf was corrected by measuring the intensity of the interference-free ^{175}Lu isotope associated with the recommended ^{176}Lu/^{175}Lu ratio of 0.02655 (Machado and Simonetti, 2001). Isotopic interference of ^{176}Yb on ^{176}Hf was corrected in a similar manner as ^{176}Lu on ^{176}Hf, using the interference-free ^{172}Yb isotope and the recommended ^{176}Yb/^{172}Yb of 0.5886 (Chu et al., 2002). Zircon 91500 was used as a reference standard with a recommended ^{176}Hf/^{177}Hf ratio of 0.282306 (Woodhead et al., 2004). One-stage model ages (T_{DM-1}) were calculated relative to the depleted mantle with a present-day (^{176}Lu/^{177}Hf)$_{DM}$ = 0.0384 and (^{176}Hf/^{177}Hf)$_{DM}$ = 0.28325 (Griffin et al., 2000). Two-stage model ages (T_{DM-2}) are calculated forcing a growth-curve through zircon initial ratio with an assumed (^{176}Lu/^{177}Hf)$_C$ ratio of 0.015 corresponding to the average continental crust (Griffin et al., 2000). Analytical results of the Lu–Hf isotopic compositions for all zircons are available in Table 1.

Totally 20 spot analyses for one sample from the ~260 Ma Baima pluton yielded relatively uniform Hf_i (0.282807–0.282897) and $\varepsilon Hf_{(T)}$ (+7.2 to +10.3) values. Ten zircons from one sample of the Taihe pluton have isotopic compositions (Hf_i = 0.282798–0.282915; $\varepsilon Hf_{(T)}$ = +6.8 to +11.0) nearly identical to that of the Baima pluton (Fig. 2).

Zircon Hf isotopic compositions of the two metaluminous plutons are slightly different from each other with a significant overlap in $\varepsilon Hf_{(T)}$ values (Fig. 2). Zircons from the ~260 Ma Woshui pluton have Hf isotopic compositions similar to those from the Baima and Taihe peralkaline plutons, with $\varepsilon Hf_{(T)}$ values between +6.1 and +13.4 and Hf_i between 0.282776 and 0.282984. Zircons from the ~252 Ma Huangcao pluton on the other hand have lower Hf_i (0.282798–0.282915) and $\varepsilon Hf_{(T)}$ (+1.5 to +8.5) values.

4. Discussion

4.1. Nature of magma source of the A-type granitic plutons in the Panxi region

A-type granitic rocks are ultimately the products of differentiation of mafic parental magmas (Turner et al., 1992; Frost and Frost, 1997; Bonin, 2007). The parental magmas may originate from different sources such as metasomatized lithospheric mantle, the lower crust, depleted mantle or enriched mantle (Eby, 1992; Poitrasson et al., 1995; Kemp et al., 2005). The metaluminous and peralkaline plutons of the Panxi region are derived from mantle rocks (Shellnutt and Zhou, 2007, 2008). The peralkaline plutons likely formed by fractional crystallization of high-Ti Emeishan flood basalts whereas the metaluminous plutons were derived by partial melting of underplated Emeishan mafic rocks which resembled an Fe- and Al-rich gabbro (Shellnutt and Zhou, 2008; Shellnutt et al., in press). The Emeishan flood basalts are subdivided into high- and low-Ti varieties and are considered to have distinct mantle sources. Although there are debates about the source of the low-Ti basalts, the high-Ti basalts are believed to be derived from an enriched mantle source (Xu et al., 2001, 2004; Xiao et al., 2004; Wang et al., 2007; Song et al., 2008; Zhou et al., 2008). Therefore the mantle source of the plutons is expected to be the same as the high-Ti flood basalts and thus an enriched mantle source (Zhong et al., 2005; Wang et al., 2007; Zhou et al., 2008). However, Xu et al. (2008) suggest the peralkaline plutons were derived from a hybrid source consisting of juvenile crust and Neoproterozoic basement rocks.

The zircon Hf isotopic compositions show that the Baima, Taihe and Woshui plutons have very similar $\varepsilon Hf_{(T)}$ (~+8.8) which suggests they originated from the same source (Fig. 2). The Huangcao pluton on the other hand is slightly different from the other plutons ($\varepsilon Hf_{(T)}$ = +5.8 ± 0.3) (Fig. 2). The whole rock Sr–Nd isotopic compositions of all the plutons have a narrow range of $\varepsilon Nd_{(T)}$ (+1.3 to +3.2), variable ^{87}Sr/$^{86}Sr_i$ ratios (0.7031–0.7099) with Sm–Nd and Rb–Sr model ages between 200 and 300 Ma (Fig. 3). The Sr–Nd compositions of the plutons fall along the mantle array and are significantly different from the basement rocks of the Yangtze Block ($\varepsilon Nd_{(T)}$ <−8.0 and $^{87}Sr/^{86}Sr_i$ >0.7090) and show no indication of crustal assimilation (Wang et al., 2007). The positive $\varepsilon Hf_{(T)}$ values (<+14) of the plutons are lower than mid-ocean ridge basalts (MORB, $\varepsilon Hf_{(T)}$ = +20) but higher than the crust (Fig. 4) (Patchett and Tatsumoto, 1980; Salters, 1996; Nowell et al., 1998; Chauvel and Blichert-Toft, 2001). Likewise, the low positive $\varepsilon Nd_{(T)}$ values (+1.3 to +3.2) contrast with the high positive $\varepsilon Nd_{(T)}$ (+10) values of MORB (i.e. depleted mantle) or negative values for the crust. The zircon Hf and whole rock Nd isotopic results suggest a source different from either the depleted mantle or the crust and indicate that the plutons had either a mixed source (e.g. depleted mantle + crust) or a homogenized enriched mantle source similar to ocean-island basalt (OIB).

Trace element ratios, such as Zr/Nb, La/Nb, Ba/Nb, Rb/Nb, Ba/La, Th/Ta and La/Yb_N ratios, do not change during differentiation and reflect the source characteristic from which the rocks were derived. The trace element ratios of the plutons are very similar to the Emeishan high-Ti basalts and overlap with enriched mantle compositions (Fig. 5) (Weaver, 1991; Xu et al., 2001; Xiao et al., 2004; Wang et al., 2007). The Th/Ta ratio is an important indicator of magma-crust interaction because mantle-derived rocks should have Th/Ta ratios of ≈2, lower than the lower continental crust (Th/Ta = 7.9) or upper continental crust (Th/Ta = 6.9). The plutons in the Panxi region have a large range of Th/Ta ratios mostly falling between 0.5 and 3.0 (Fig. 5e). The metaluminous plutons however, show higher Ba/Nb and Ba/La ratios than the high-Ti basaltic rocks which may be due to either low degrees of partial melting or melting from Ba-rich rocks (Fig. 5b and d) (Shellnutt and Zhou, 2007, 2008). In any case the trace elements ratios of the A-type granitic plutons of the Panxi region do not show evidence for significant crustal assimilation.

The $\varepsilon Hf_{(T)}$ and $\varepsilon Nd_{(T)}$ values of the A-type granitic plutons fall along the mantle array and are very similar to Hawaiian volcanic rocks ($\varepsilon Hf_{(T)}$ = 4.4–14.4) and ocean-island basalt (Fig. 4) (Blichert-Toft et al., 1999; Kempton et al., 2000; Chauvel et al., 2008). Because there is little or no evidence for crustal assimilation and the fact that the trace element ratios eliminate the possibility of a pure depleted mantle source, we are left to conclude that the $\varepsilon Hf_{(T)}$ values of all the plutons are indicative of the original source magma and thus enriched mantle. Enriched mantle implies that there is subducted material or a 'recycled component' in the source, however this does not mean that there was late stage assimilation of Yangtze Block material (Chauvel et al., 2008).

Table 1
Zircon Hf isotopic results.

Sample	Pluton	$^{176}Hf/^{177}Hf$	2σ	$^{176}Lu/^{177}Hf$	$^{176}Yb/^{177}Hf$	$Hf_{initial}$	$\varepsilon Hf_{(T)}$	1σ	T_{DM-1} (Ga)	T_{DM-2} (Ga)
GS05-062-1	Huangcao	0.282727	0.00002	0.0025	0.0918	0.28272	+3.7	0.4	0.75	1.02
GS05-062-2	Huangcao	0.282797	0.00002	0.0005	0.0181	0.28280	+6.5	0.3	0.62	0.84
GS05-062-3	Huangcao	0.282757	0.00002	0.0022	0.0852	0.28275	+4.8	0.3	0.70	0.95
GS05-062-4	Huangcao	0.282781	0.00002	0.0011	0.0395	0.28278	+5.9	0.4	0.65	0.89
GS05-062-5	Huangcao	0.282796	0.00002	0.0006	0.0224	0.28279	+6.5	0.3	0.62	0.85
GS05-062-6	Huangcao	0.282744	0.00003	0.0005	0.0210	0.28274	+4.6	0.6	0.69	0.96
GS05-062-7	Huangcao	0.282837	0.00003	0.0009	0.0375	0.28283	+7.9	0.5	0.57	0.76
GS05-062-8	Huangcao	0.282792	0.00002	0.0003	0.0122	0.28279	+6.4	0.4	0.62	0.85
GS05-062-9	Huangcao	0.282764	0.00002	0.0021	0.0848	0.28275	+5.1	0.4	0.69	0.94
GS05-062-10	Huangcao	0.282775	0.00002	0.0004	0.0185	0.28277	+5.8	0.3	0.64	0.89
GS05-062-11	Huangcao	0.282754	0.00002	0.0012	0.0508	0.28275	+4.9	0.4	0.69	0.95
GS05-062-12	Huangcao	0.282819	0.00002	0.0011	0.0481	0.28281	+7.2	0.3	0.60	0.80
GS05-062-13	Huangcao	0.282774	0.00002	0.0008	0.0374	0.28277	+5.6	0.4	0.65	0.90
GS05-062-14	Huangcao	0.282827	0.00003	0.0003	0.0117	0.28283	+7.6	0.5	0.57	0.78
GS05-062-15	Huangcao	0.282806	0.00003	0.0018	0.0743	0.28280	+6.6	0.4	0.62	0.84
GS05-062-16	Huangcao	0.282770	0.00003	0.0028	0.1029	0.28276	+5.2	0.5	0.69	0.93
GS05-062-17	Huangcao	0.282787	0.00002	0.0025	0.1096	0.28278	+5.8	0.4	0.66	0.89
GS05-062-18	Huangcao	0.282775	0.00002	0.0007	0.0296	0.28277	+5.7	0.3	0.65	0.89
GS05-062-19	Huangcao	0.282792	0.00002	0.0009	0.0341	0.28279	+6.3	0.4	0.63	0.86
GS05-062-20	Huangcao	0.282802	0.00003	0.0007	0.0286	0.28280	+6.7	0.5	0.61	0.83
GS05-062-21	Huangcao	0.282768	0.00003	0.0002	0.0079	0.28277	+5.5	0.5	0.65	0.91
GS05-062-22	Huangcao	0.282784	0.00003	0.0004	0.0186	0.28278	+6.1	0.5	0.63	0.87
GS05-062-23	Huangcao	0.282831	0.00003	0.0012	0.0531	0.28283	+7.6	0.4	0.58	0.78
GS05-062-24	Huangcao	0.282764	0.00002	0.0006	0.0230	0.28276	+5.3	0.4	0.66	0.92
GS05-062-25	Huangcao	0.282810	0.00003	0.0015	0.0697	0.28280	+6.8	0.5	0.62	0.83
GS05-060-1	Huangcao	0.282770	0.00002	0.0010	0.0372	0.28277	+5.5	0.3	0.66	0.91
GS05-060-2	Huangcao	0.282784	0.00002	0.0015	0.0551	0.28278	+5.9	0.4	0.65	0.88
GS05-060-3	Huangcao	0.282770	0.00002	0.0009	0.0296	0.28277	+5.5	0.3	0.66	0.91
GS05-060-4	Huangcao	0.282747	0.00002	0.0027	0.1298	0.28273	+4.4	0.4	0.72	0.98
GS05-060-5	Huangcao	0.282784	0.00002	0.0010	0.0382	0.28278	+6.0	0.3	0.64	0.88
GS05-060-6	Huangcao	0.282771	0.00002	0.0008	0.0317	0.28277	+5.6	0.3	0.66	0.90
GS05-060-7	Huangcao	0.282841	0.00002	0.0017	0.0660	0.28283	+7.9	0.4	0.57	0.76
GS05-060-8	Huangcao	0.282773	0.00002	0.0016	0.0840	0.28277	+5.5	0.3	0.67	0.91
GS05-060-9	Huangcao	0.282779	0.00002	0.0008	0.0334	0.28278	+5.8	0.3	0.64	0.89
GS05-060-10	Huangcao	0.282781	0.00003	0.0005	0.0203	0.28278	+6.0	0.4	0.64	0.88
GS05-060-11	Huangcao	0.282845	0.00003	0.0017	0.0769	0.28284	+8.0	0.5	0.57	0.75
GS05-060-12	Huangcao	0.282754	0.00002	0.0014	0.0584	0.28275	+4.9	0.4	0.69	0.95
GS05-060-13	Huangcao	0.282759	0.00003	0.0008	0.0334	0.28276	+5.1	0.5	0.67	0.93
GS05-060-14	Huangcao	0.282745	0.00002	0.0008	0.0332	0.28274	+4.7	0.4	0.69	0.96
GS05-060-15	Huangcao	0.282771	0.00002	0.0010	0.0473	0.28277	+5.5	0.4	0.66	0.91
GS05-060-16	Huangcao	0.282769	0.00003	0.0008	0.0373	0.28277	+5.5	0.6	0.66	0.91
GS05-060-17	Huangcao	0.282824	0.00002	0.0013	0.0728	0.28282	+7.3	0.4	0.59	0.80
GS05-060-18	Huangcao	0.282778	0.00003	0.0004	0.0194	0.28278	+5.9	0.5	0.64	0.89
GS05-060-19	Huangcao	0.282773	0.00003	0.0008	0.0360	0.28277	+5.6	0.4	0.65	0.90
GS05-060-20	Huangcao	0.282730	0.00003	0.0017	0.0964	0.28272	+3.9	0.4	0.73	1.01
GS05-060-21	Huangcao	0.282766	0.00002	0.0009	0.0533	0.28276	+5.3	0.3	0.67	0.92
GS05-060-22	Huangcao	0.282836	0.00002	0.0012	0.0512	0.28283	+7.8	0.4	0.57	0.77
GS05-060-23	Huangcao	0.282658	0.00003	0.0014	0.0424	0.28265	+1.5	0.6	0.82	1.16
GS05-060-24	Huangcao	0.282750	0.00003	0.0023	0.1139	0.28274	+4.5	0.5	0.71	0.97
GS05-060-25	Huangcao	0.282764	0.00003	0.0011	0.0488	0.28276	+5.3	0.5	0.67	0.92
GS05-059-1	Huangcao	0.282864	0.00002	0.0029	0.1212	0.28285	+8.5	0.4	0.56	0.72
GS05-059-2	Huangcao	0.282809	0.00002	0.0010	0.0368	0.28280	+6.9	0.4	0.61	0.82
GS05-059-3	Huangcao	0.282785	0.00003	0.0024	0.0842	0.28277	+5.8	0.4	0.66	0.89
GS05-059-4	Huangcao	0.282850	0.00003	0.0041	0.1501	0.28283	+7.8	0.4	0.60	0.77
GS05-059-5	Huangcao	0.282828	0.00003	0.0028	0.1005	0.28281	+7.2	0.5	0.61	0.80
GS05-059-6	Huangcao	0.282770	0.00002	0.0029	0.0923	0.28276	+5.2	0.4	0.69	0.93
GS05-059-7	Huangcao	0.282798	0.00003	0.0019	0.0732	0.28279	+6.3	0.5	0.64	0.86
GS05-059-8	Huangcao	0.282789	0.00002	0.0006	0.0216	0.28279	+6.2	0.4	0.63	0.86
GS05-059-9	Huangcao	0.282844	0.00003	0.0010	0.0409	0.28284	+8.1	0.4	0.56	0.75
GS05-059-10	Huangcao	0.282848	0.00003	0.0005	0.0184	0.28285	+8.3	0.5	0.55	0.73
GS05-059-11	Huangcao	0.282815	0.00002	0.0009	0.0366	0.28281	+7.1	0.4	0.60	0.81
GS05-059-12	Huangcao	0.282779	0.00003	0.0029	0.1106	0.28277	+5.5	0.5	0.68	0.91
GS05-059-13	Huangcao	0.282730	0.00003	0.0008	0.0301	0.28273	+4.1	0.5	0.71	0.99
GS05-059-14	Huangcao	0.282830	0.00002	0.0027	0.1146	0.28282	+7.3	0.4	0.61	0.80
GS05-059-15	Huangcao	0.282806	0.00003	0.0034	0.1520	0.28279	+6.3	0.4	0.65	0.86
GS05-059-16	Huangcao	0.282793	0.00002	0.0016	0.0633	0.28279	+6.2	0.4	0.64	0.87
GS05-059-17	Huangcao	0.282828	0.00002	0.0018	0.0705	0.28282	+7.4	0.4	0.59	0.79
GS05-059-18	Huangcao	0.282826	0.00003	0.0026	0.1092	0.28281	+7.2	0.5	0.61	0.80
GS05-059-19	Huangcao	0.282753	0.00002	0.0025	0.1063	0.28274	+4.6	0.4	0.71	0.96
GS05-059-20	Huangcao	0.282802	0.00002	0.0022	0.0915	0.28279	+6.4	0.4	0.64	0.85
GS05-059-21	Huangcao	0.282831	0.00003	0.0017	0.0664	0.28282	+7.5	0.5	0.59	0.78
GS05-059-22	Huangcao	0.282780	0.00002	0.0006	0.0222	0.28278	+5.9	0.3	0.64	0.88
GS05-059-23	Huangcao	0.282800	0.00002	0.0014	0.0550	0.28279	+6.5	0.4	0.63	0.85
GS05-059-24	Huangcao	0.282748	0.00002	0.0019	0.0639	0.28274	+4.5	0.4	0.71	0.97
GS05-059-25	Huangcao	0.282784	0.00002	0.0005	0.0206	0.28278	+6.1	0.3	0.63	0.87

Table 1 (*continued*)

Sample	Pluton	$^{176}Hf/^{177}Hf$	2σ	$^{176}Lu/^{177}Hf$	$^{176}Yb/^{177}Hf$	$Hf_{initial}$	$\varepsilon Hf_{(T)}$	1σ	T_{DM-1} (Ga)	T_{DM-2} (Ga)
GS05-047-1	Woshui	0.282843	0.00002	0.0018	0.0724	0.28283	+8.1	0.4	0.57	0.75
GS05-047-2	Woshui	0.282822	0.00002	0.0006	0.0235	0.28282	7.6	0.3	0.58	0.79
GS05-047-3	Woshui	0.282890	0.00003	0.0038	0.1627	0.28287	+9.4	0.5	0.53	0.67
GS05-047-4	Woshui	0.282870	0.00002	0.0008	0.0330	0.28287	+9.2	0.4	0.52	0.68
GS05-047-5	Woshui	0.282890	0.00002	0.0020	0.0857	0.28288	+9.7	0.4	0.51	0.65
GS05-047-6	Woshui	0.282830	0.00002	0.0021	0.0957	0.28282	+7.6	0.4	0.60	0.78
GS05-047-7	Woshui	0.282881	0.00002	0.0014	0.0602	0.28287	+9.5	0.4	0.51	0.67
GS05-047-8	Woshui	0.282812	0.00002	0.0024	0.0837	0.28280	+6.9	0.4	0.63	0.83
GS05-047-9	Woshui	0.282801	0.00003	0.0023	0.0782	0.28279	+6.5	0.5	0.64	0.85
GS05-047-10	Woshui	0.282887	0.00002	0.0021	0.1047	0.28288	+9.6	0.4	0.52	0.66
GS05-047-11	Woshui	0.282787	0.00002	0.0021	0.0997	0.28278	+6.1	0.4	0.66	0.88
GS05-047-12	Woshui	0.282882	0.00002	0.0015	0.0713	0.28287	+9.5	0.4	0.51	0.66
GS05-047-13	Woshui	0.282838	0.00002	0.0006	0.0288	0.28284	+8.1	0.3	0.56	0.75
GS05-047-14	Woshui	0.282864	0.00002	0.0007	0.0311	0.28286	+9.1	0.4	0.53	0.69
GS05-047-15	Woshui	0.282833	0.00002	0.0006	0.0296	0.28283	+8.0	0.4	0.57	0.76
GS05-047-16	Woshui	0.282873	0.00003	0.0016	0.0519	0.28287	+9.2	0.5	0.53	0.69
GS05-047-17	Woshui	0.282849	0.00003	0.0010	0.0427	0.28284	+8.5	0.4	0.55	0.73
GS05-047-18	Woshui	0.282838	0.00003	0.0015	0.0652	0.28283	+8.0	0.5	0.57	0.76
GS05-047-19	Woshui	0.282903	0.00003	0.0041	0.1642	0.28288	+9.8	0.5	0.52	0.65
GS05-047-20	Woshui	0.282849	0.00003	0.0018	0.0595	0.28284	+8.3	0.5	0.56	0.74
GS05-047-21	Woshui	0.282967	0.00004	0.0026	0.1054	0.28295	+12.4	0.6	0.41	0.49
GS05-047-22	Woshui	0.282847	0.00002	0.0009	0.0459	0.28284	+8.4	0.4	0.55	0.74
GS05-047-23	Woshui	0.282899	0.00003	0.0026	0.1201	0.28289	+9.9	0.4	0.51	0.64
GS05-047-24	Woshui	0.282891	0.00003	0.0009	0.0383	0.28289	+10.0	0.5	0.49	0.64
GS05-047-25	Woshui	0.282859	0.00002	0.0008	0.0349	0.28286	+8.8	0.4	0.54	0.71
GS05-049-1	Woshui	0.282828	0.00002	0.0029	0.1133	0.28281	+7.4	0.4	0.61	0.80
GS05-049-2	Woshui	0.282851	0.00002	0.0008	0.0336	0.28285	+8.6	0.3	0.55	0.73
GS05-049-3	Woshui	0.282865	0.00002	0.0009	0.0367	0.28286	+9.0	0.4	0.53	0.70
GS05-049-4	Woshui	0.282783	0.00002	0.0011	0.0464	0.28278	+6.1	0.3	0.64	0.88
GS05-049-5	Woshui	0.282851	0.00002	0.0007	0.0291	0.28285	+8.6	0.4	0.55	0.72
GS05-049-6	Woshui	0.282886	0.00002	0.0017	0.0749	0.28288	+9.6	0.4	0.51	0.66
GS05-049-7	Woshui	0.282862	0.00002	0.0018	0.0719	0.28285	+8.8	0.4	0.55	0.71
GS05-049-8	Woshui	0.282815	0.00002	0.0003	0.0084	0.28281	+7.4	0.3	0.59	0.80
GS05-049-9	Woshui	0.282849	0.00002	0.0008	0.0360	0.28284	+8.5	0.4	0.55	0.73
GS05-049-10	Woshui	0.282878	0.00002	0.0009	0.0390	0.28287	+9.5	0.4	0.51	0.67
GS05-049-11	Woshui	0.282835	0.00002	0.0019	0.0877	0.28283	+7.8	0.4	0.59	0.77
GS05-049-12	Woshui	0.282846	0.00002	0.0023	0.1026	0.28283	+8.1	0.4	0.58	0.75
GS05-049-13	Woshui	0.282867	0.00002	0.0011	0.0417	0.28286	+9.1	0.3	0.53	0.69
GS05-049-14	Woshui	0.282891	0.00002	0.0016	0.0708	0.28288	+9.8	0.4	0.50	0.65
GS05-049-15	Woshui	0.282870	0.00003	0.0015	0.0636	0.28286	+9.1	0.4	0.53	0.69
GS05-049-16	Woshui	0.282803	0.00003	0.0014	0.0635	0.28280	+6.7	0.4	0.62	0.84
GS05-049-17	Woshui	0.282878	0.00002	0.0007	0.0334	0.28287	+9.5	0.4	0.51	0.66
GS05-049-18	Woshui	0.282887	0.00002	0.0011	0.0466	0.28288	+9.8	0.4	0.50	0.65
GS05-049-19	Woshui	0.282854	0.00003	0.0023	0.1051	0.28284	+8.4	0.5	0.57	0.73
GS05-049-20	Woshui	0.282849	0.00002	0.0004	0.0168	0.28285	+8.5	0.4	0.54	0.72
GS05-049-21	Woshui	0.282896	0.00003	0.0007	0.0312	0.28289	+10.2	0.4	0.48	0.62
GS05-049-22	Woshui	0.282815	0.00002	0.0011	0.0415	0.28281	+7.3	0.3	0.60	0.81
GS05-049-23	Woshui	0.282855	0.00002	0.0011	0.0485	0.28285	+8.6	0.3	0.55	0.72
GS05-049-24	Woshui	0.282853	0.00002	0.0009	0.0428	0.28285	+8.6	0.4	0.55	0.72
GS05-049-25	Woshui	0.282827	0.00002	0.0024	0.1204	0.28282	+7.4	0.4	0.60	0.79
GS05-064-1	Woshui	0.282860	0.00002	0.0012	0.0595	0.28285	+8.8	0.4	0.54	0.71
GS05-064-2	Woshui	0.282900	0.00002	0.0020	0.0723	0.28289	+10.1	0.4	0.50	0.63
GS05-064-3	Woshui	0.282835	0.00002	0.0012	0.0434	0.28283	+7.9	0.3	0.58	0.77
GS05-064-4	Woshui	0.282873	0.00002	0.0020	0.0786	0.28286	+9.1	0.4	0.53	0.69
GS05-064-5	Woshui	0.282867	0.00003	0.0010	0.0379	0.28286	+9.1	0.4	0.53	0.69
GS05-064-6	Woshui	0.282920	0.00003	0.0009	0.0317	0.28292	+11.0	0.4	0.45	0.57
GS05-064-7	Woshui	0.282846	0.00003	0.0014	0.0508	0.28284	+8.3	0.5	0.56	0.74
GS05-064-8	Woshui	0.282864	0.00003	0.0012	0.0430	0.28286	+9.0	0.4	0.53	0.70
GS05-064-9	Woshui	0.282896	0.00002	0.0015	0.0582	0.28289	+10.0	0.4	0.49	0.63
GS05-064-10	Woshui	0.282886	0.00003	0.0014	0.0476	0.28288	+9.7	0.5	0.51	0.65
GS05-064-11	Woshui	0.282858	0.00002	0.0008	0.0453	0.28285	+8.8	0.3	0.54	0.71
GS05-064-12	Woshui	0.282822	0.00003	0.0008	0.0265	0.28282	+7.5	0.5	0.59	0.79
GS05-064-13	Woshui	0.282829	0.00003	0.0009	0.0298	0.28283	+7.8	0.4	0.58	0.77
GS05-064-14	Woshui	0.282887	0.00003	0.0014	0.0496	0.28288	+9.7	0.5	0.51	0.65
GS05-064-15	Woshui	0.282897	0.00003	0.0014	0.0478	0.28289	+10.1	0.4	0.49	0.63
GS05-064-16	Woshui	0.282852	0.00002	0.0014	0.0489	0.28285	+8.5	0.4	0.55	0.73
GS05-064-17	Woshui	0.282935	0.00004	0.0018	0.0704	0.28293	+11.3	0.7	0.44	0.55
GS05-064-18	Woshui	0.282861	0.00002	0.0016	0.0600	0.28285	+8.8	0.4	0.54	0.71
GS05-064-19	Woshui	0.282826	0.00002	0.0013	0.0495	0.28282	+7.6	0.4	0.59	0.78
GS05-064-20	Woshui	0.282863	0.00003	0.0018	0.0664	0.28285	+8.8	0.4	0.54	0.71
GS05-064-21	Woshui	0.282853	0.00002	0.0011	0.0372	0.28285	+8.6	0.5	0.55	0.72
GS05-067-1	Woshui	0.282856	0.00003	0.0014	0.0498	0.28285	+8.6	0.6	0.55	0.72
GS05-067-2	Woshui	0.282889	0.00003	0.0005	0.0187	0.28289	+9.9	0.5	0.49	0.64
GS05-067-3	Woshui	0.282888	0.00003	0.0013	0.0478	0.28288	+9.8	0.6	0.50	0.65
GS05-067-4	Woshui	0.282879	0.00002	0.0013	0.0526	0.28287	+9.5	0.4	0.52	0.67
GS05-067-5	Woshui	0.282912	0.00002	0.0017	0.0622	0.28290	+10.6	0.4	0.47	0.60

(*continued on next page*)

Table 1 (*continued*)

Sample	Pluton	$^{176}Hf/^{177}Hf$	2σ	$^{176}Lu/^{177}Hf$	$^{176}Yb/^{177}Hf$	$Hf_{initial}$	$\varepsilon Hf_{(T)}$	1σ	T_{DM-1} (Ga)	T_{DM-2} (Ga)
GS05-067-6	Woshui	0.282867	0.00002	0.0013	0.0481	0.28286	+9.1	0.4	0.53	0.69
GS05-067-7	Woshui	0.282916	0.00003	0.0013	0.0466	0.28291	10.8	0.5	0.46	0.59
GS05-067-8	Woshui	0.282865	0.00002	0.0009	0.0355	0.28286	+9.0	0.4	0.53	0.70
GS05-067-9	Woshui	0.282895	0.00003	0.0013	0.0463	0.28289	+10.0	0.5	0.49	0.63
GS05-067-10	Woshui	0.282853	0.00003	0.0006	0.0226	0.28285	+8.7	0.5	0.54	0.72
GS05-067-11	Woshui	0.282845	0.00004	0.0013	0.0447	0.28284	+8.3	0.7	0.56	0.74
GS05-067-12	Woshui	0.282892	0.00003	0.0004	0.0120	0.28289	+10.1	0.5	0.49	0.63
GS05-067-13	Woshui	0.282829	0.00003	0.0015	0.0541	0.28282	+7.7	0.5	0.59	0.78
GS05-067-14	Woshui	0.282842	0.00002	0.0013	0.0551	0.28284	+8.1	0.4	0.57	0.75
GS05-067-15	Woshui	0.282879	0.00003	0.0017	0.0594	0.28287	+9.4	0.5	0.52	0.67
GS05-067-16	Woshui	0.282855	0.00002	0.0009	0.0322	0.28285	+8.7	0.4	0.54	0.72
GS05-067-17	Woshui	0.282927	0.00003	0.0017	0.0606	0.28292	+11.1	0.5	0.45	0.57
GS05-067-18	Woshui	0.282884	0.00002	0.0013	0.0487	0.28288	+9.6	0.4	0.51	0.66
GS05-067-19	Woshui	0.282889	0.00003	0.0015	0.0563	0.28288	+9.8	0.5	0.50	0.65
GS05-067-20	Woshui	0.282814	0.00003	0.0007	0.0244	0.28281	+7.3	0.5	0.60	0.80
GS05-067-21	Woshui	0.282855	0.00002	0.0009	0.0298	0.28285	+8.7	0.4	0.54	0.72
GS03-120-1	Woshui	0.282837	0.00003	0.0010	0.0338	0.28283	+8.0	0.5	0.57	0.76
GS03-120-2	Woshui	0.282927	0.00003	0.0012	0.0403	0.28292	+11.2	0.5	0.45	0.56
GS03-120-3	Woshui	0.282912	0.00002	0.0007	0.0234	0.28291	+10.7	0.4	0.46	0.59
GS03-120-4	Woshui	0.282870	0.00003	0.0013	0.0489	0.28286	+9.2	0.4	0.53	0.69
GS03-120-5	Woshui	0.282895	0.00003	0.0018	0.0619	0.28289	+9.9	0.5	0.50	0.64
GS03-120-6	Woshui	0.282872	0.00002	0.0006	0.0214	0.28287	+9.3	0.4	0.52	0.68
GS03-120-7	Woshui	0.282865	0.00003	0.0007	0.0243	0.28286	+9.1	0.5	0.53	0.69
GS03-120-8	Woshui	0.282867	0.00003	0.0021	0.0743	0.28286	+8.9	0.5	0.54	0.70
GS03-120-9	Woshui	0.282860	0.00003	0.0009	0.0394	0.28286	+8.9	0.4	0.54	0.71
GS03-120-10	Woshui	0.282902	0.00003	0.0004	0.0135	0.28290	+10.5	0.5	0.47	0.61
GS03-120-11	Woshui	0.282851	0.00002	0.0006	0.0214	0.28285	+8.6	0.4	0.54	0.72
GS03-120-12	Woshui	0.282886	0.00004	0.0011	0.0430	0.28288	+9.8	0.7	0.50	0.65
GS03-120-13	Woshui	0.282844	0.00003	0.0014	0.0556	0.28284	+8.2	0.5	0.56	0.75
GS03-120-14	Woshui	0.282855	0.00003	0.0013	0.0525	0.28285	8.6	0.5	0.55	0.72
GS03-120-15	Woshui	0.282853	0.00003	0.0013	0.0543	0.28285	+8.6	0.5	0.55	0.73
GS03-120-16	Woshui	0.282857	0.00003	0.0005	0.0191	0.28285	+8.8	0.5	0.54	0.71
GS03-120-17	Woshui	0.282908	0.00003	0.0004	0.0171	0.28291	+10.6	0.5	0.46	0.60
GS03-120-18	Woshui	0.282886	0.00003	0.0004	0.0154	0.28288	+9.9	0.5	0.49	0.64
GS03-120-19	Woshui	0.282986	0.00005	0.0006	0.0200	0.28298	13.4	0.9	0.36	0.42
GS03-120-20	Woshui	0.282861	0.00002	0.0005	0.0209	0.28286	+9.0	0.4	0.53	0.70
GS03-120-21	Woshui	0.282861	0.00003	0.0008	0.0311	0.28286	+8.9	0.5	0.53	0.70
GS03-120-22	Woshui	0.282822	0.00003	0.0005	0.0203	0.28282	+7.6	0.5	0.58	0.78
GS03-120-23	Woshui	0.282881	0.00003	0.0015	0.0603	0.28287	+9.5	0.5	0.52	0.67
GS05-004-1	Baima	0.282924	0.00003	0.0055	0.2910	0.28290	+10.3	0.4	0.51	0.62
GS05-004-2	Baima	0.282854	0.00002	0.0007	0.0315	0.28285	+8.7	0.4	0.54	0.72
GS05-004-3	Baima	0.282810	0.00002	0.0006	0.0266	0.28281	+7.2	0.3	0.60	0.81
GS05-004-4	Baima	0.282867	0.00002	0.0009	0.0400	0.28286	+9.1	0.3	0.53	0.69
GS05-004-5	Baima	0.282891	0.00003	0.0015	0.0710	0.28288	+9.9	0.5	0.50	0.64
GS05-004-6	Baima	0.282854	0.00002	0.0010	0.0448	0.28285	+8.6	0.4	0.55	0.72
GS05-004-7	Baima	0.282886	0.00002	0.0007	0.0335	0.28288	+9.8	0.4	0.50	0.65
GS05-004-8	Baima	0.282878	0.00002	0.0015	0.0706	0.28287	+9.4	0.4	0.52	0.67
GS05-004-9	Baima	0.282851	0.00002	0.0008	0.0433	0.28285	+8.5	0.3	0.55	0.73
GS05-004-10	Baima	0.282852	0.00002	0.0005	0.0255	0.28285	+8.6	0.4	0.54	0.72
GS05-004-11	Baima	0.282888	0.00002	0.0018	0.0916	0.28288	+9.7	0.4	0.51	0.66
GS05-004-12	Baima	0.282860	0.00002	0.0013	0.0667	0.28285	+8.8	0.4	0.54	0.71
GS05-004-13	Baima	0.282850	0.00003	0.0011	0.0554	0.28284	+8.5	0.4	0.55	0.73
GS05-004-14	Baima	0.282835	0.00002	0.0011	0.0522	0.28283	+7.9	0.4	0.57	0.76
GS05-004-15	Baima	0.282858	0.00002	0.0006	0.0284	0.28285	+8.8	0.4	0.54	0.71
GS05-004-16	Baima	0.282861	0.00002	0.0008	0.0322	0.28286	+8.9	0.4	0.53	0.70
GS05-004-17	Baima	0.282869	0.00003	0.0008	0.0351	0.28287	+9.2	0.4	0.52	0.69
GS05-004-18	Baima	0.282861	0.00002	0.0010	0.0434	0.28286	+8.9	0.4	0.54	0.71
GS05-004-19	Baima	0.282903	0.00003	0.0012	0.0555	0.28290	+10.3	0.5	0.48	0.62
GS05-004-20	Baima	0.282862	0.00002	0.0019	0.0791	0.28285	+8.8	0.4	0.55	0.71
GS04-155-1	Taihe	0.282871	0.00003	0.0012	0.0573	0.28287	+9.2	0.6	0.52	0.68
GS04-155-2	Taihe	0.282928	0.00003	0.0026	0.1097	0.28292	+11.0	0.5	0.46	0.57
GS04-155-3	Taihe	0.282889	0.00003	0.0025	0.1199	0.28288	+9.6	0.5	0.52	0.66
GS04-155-4	Taihe	0.282843	0.00003	0.0019	0.1018	0.28283	+8.1	0.4	0.57	0.76
GS04-155-5	Taihe	0.282813	0.00003	0.0031	0.1516	0.28280	+6.8	0.5	0.64	0.83
GS04-155-6	Taihe	0.282849	0.00002	0.0016	0.0836	0.28284	+8.4	0.4	0.56	0.74
GS04-155-7	Taihe	0.282915	0.00002	0.0015	0.0694	0.28291	+10.7	0.4	0.47	0.59
GS04-155-8	Taihe	0.282911	0.00002	0.0015	0.0725	0.28290	+10.6	0.4	0.47	0.60
GS04-155-9	Taihe	0.282916	0.00003	0.0010	0.0506	0.28291	+10.8	0.4	0.46	0.58
GS04-155-10	Taihe	0.282845	0.00002	0.0010	0.0499	0.28284	+8.3	0.4	0.56	0.74
91500	Standard	0.282292		0.0003	0.0120	0.28229	−11.1	0.7	1.29	1.93
91500	Standard	0.282301		0.0003	0.0110	0.28230	−10.8	0.6	1.27	1.91
91500	Standard	0.282303		0.0003	0.0100	0.28230	−10.7	0.7	1.27	1.91
91500	Standard	0.282298		0.0003	0.0100	0.28230	−10.9	0.7	1.28	1.92
91500	Standard	0.282364		0.0003	0.0100	0.28236	−8.6	0.7	1.19	1.78
91500	Standard	0.282315		0.0003	0.0110	0.28231	−10.3	0.8	1.26	1.88
91500	Standard	0.282258		0.0003	0.0110	0.28226	−12.3	0.8	1.33	2.00

Table 1 (*continued*)

Sample	Pluton	$^{176}Hf/^{177}Hf$	2σ	$^{176}Lu/^{177}Hf$	$^{176}Yb/^{177}Hf$	$Hf_{initial}$	$\varepsilon Hf_{(T)}$	1σ	T_{DM-1} (Ga)	T_{DM-2} (Ga)
91500	Standard	0.282327		0.0003	0.0100	0.28233	−9.9	0.7	1.24	1.86
91500	Standard	0.282270		0.0003	0.0100	0.28227	−11.9	0.7	1.32	1.98
91500	Standard	0.282324		0.0003	0.0090	0.28232	−10.0	0.7	1.25	1.86
91500	Standard	0.282287		0.0003	0.0090	0.28229	−11.3	0.6	1.29	1.94
91500	Standard	0.282310		0.0003	0.0090	0.28231	−10.5	0.7	1.26	1.89
91500	Standard	0.282290		0.0003	0.0090	0.28229	−11.2	0.7	1.29	1.94
91500	Standard	0.282403		0.0003	0.0100	0.28240	−7.2	1.6	1.14	1.69
91500	Standard	0.282222		0.0003	0.0100	0.28222	−13.6	1.7	1.38	2.08
91500	Standard	0.282325		0.0003	0.0080	0.28232	−10.0	1.7	1.24	1.86
91500	Standard	0.282279		0.0003	0.0080	0.28228	−11.6	1.7	1.30	1.96
91500	Standard	0.282256		0.0003	0.0080	0.28225	−12.4	1.6	1.33	2.01
91500	Standard	0.282278		0.0003	0.0080	0.28228	−11.6	1.8	1.31	1.96
91500	Standard	0.282373		0.0003	0.0080	0.28237	−8.3	1.8	1.18	1.76
91500	Standard	0.282329		0.0003	0.0080	0.28233	−9.8	1.7	1.24	1.85

$T_{DM-1} = (1/0.01865)^{*} \ln((1 + (^{176}Hf/^{177}Hf - 0.28325)/(^{176}Lu/^{177}Hf - 0.0384))$. $T_{DM-2} = (Age/1000) + ((1/0.01865)^{*} \ln(1 + (Hf_i - Hf_{DM(t)})/(0.015 - 0.0384)))$.

Zircon $\varepsilon Hf_{(T)}$ values of the ~252 Ma Huangcao pluton are generally lower than those of the Baima, Taihe and Woshui plutons. The Huangcao pluton has Sr–Nd isotopic values and trace element ratios similar to the other plutons (e.g. low Th/Ta and $\varepsilon Nd_{(T)} = +1.3$ to +1.9). The longer crustal residency time of the Huangcao pluton source rocks may be the reason for the lower zircon $\varepsilon Hf_{(T)}$ values. The zircon Hf data of the Huangcao pluton are difficult to interpret because if they are indicative of a mixed source (e.g. crust + depleted mantle), then why were the bulk rock trace element (e.g. no negative Nb–Ta anomalies) and Sr–Nd (e.g. positive $\varepsilon Nd_{(T)}$) composition unaffected by crustal assimilation? It seems very unlikely that crustal assimilation would only affect the zircon Hf isotopic values. The lower $\varepsilon Hf_{(T)}$ value may simply be related to fractionation of Lu relative to Hf. If the source rocks of the Huangcao pluton had experienced a previous melting event then it is conceivable that the lower $\varepsilon Hf_{(T)}$ values were a result of preferential partition of Lu relative to Hf in zircon during the early melting event (Kinny and Maas, 2003; Shellnutt and Zhou, 2008). Considering the available evidence, we believe it is doubtful that there was significant crustal assimilation during the genesis of the Huangcao pluton and that the zircon Hf isotopic values are characteristic of the magma source.

Previous zircon Hf isotope studies of ELIP felsic plutonic rocks (e.g. Maomaogou Miyi, Taihe, Salian and Ailanghe plutons) by Xu et al. (2008) show variable $\varepsilon Hf_{(T)}$ values ($\varepsilon Hf_{(T)} = -4.4$ to +13.4) and Hf model ages ($T_{DM-1} = 440–1790$ Ma) which were interpreted as evidence for a mixed mantle (i.e. juvenile crust) and crust (Neoproterozoic crust) source. Although the Maomaogou, Miyi

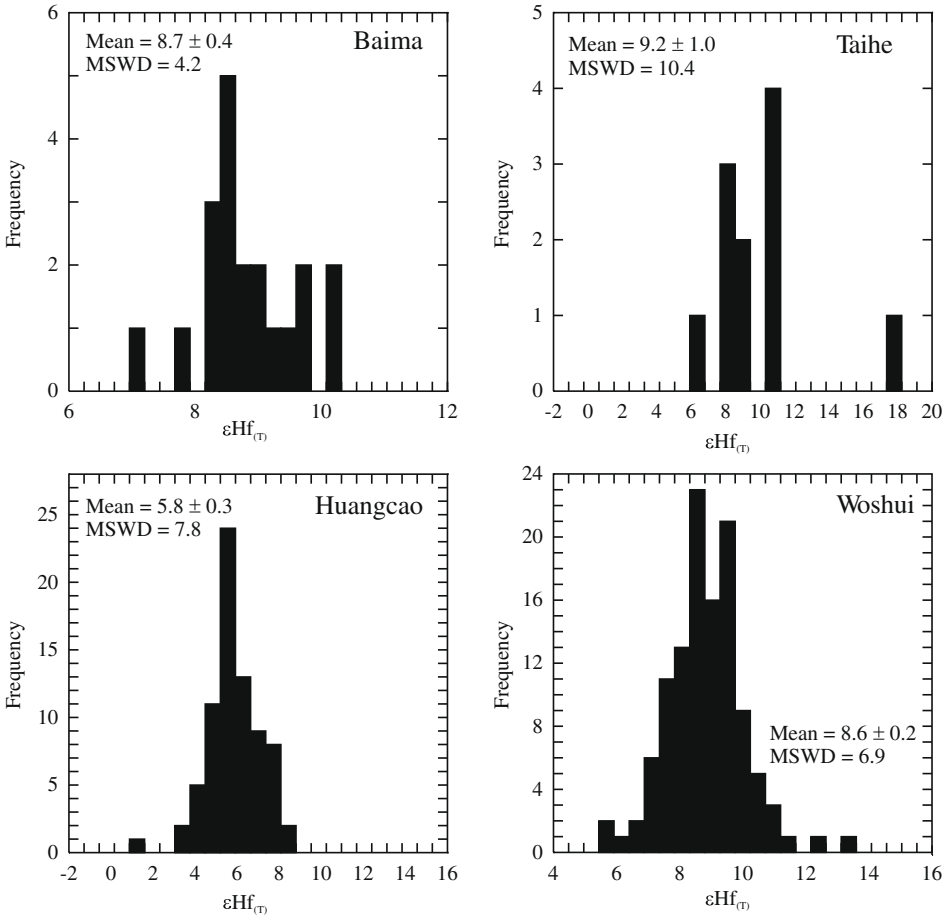

Fig. 2. Frequency distribution of the zircon $\varepsilon Hf_{(T)}$ values for the Panxi plutons. Weighted mean values and mean square of weighted deviates are reported for each.

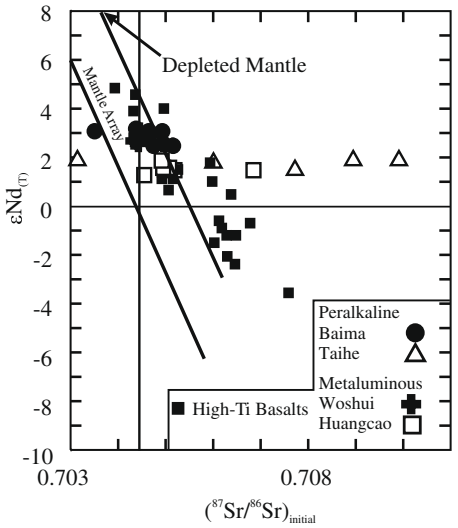

Fig. 3. $\varepsilon Nd_{(T)}$ vs. $^{87}Sr/^{86}Sr_i$ of the A-type granitic plutons of the Panxi region granitoids and Emeishan high-Ti basaltic rocks. Data from Xu et al. (2001), Zhou et al. (2006) and Shellnutt and Zhou (2007, 2008). The $^{87}Sr/^{86}Sr_i$ values for the peralkaline have been calculated to their Rb–Sr isochron age and used for comparison purposes only.

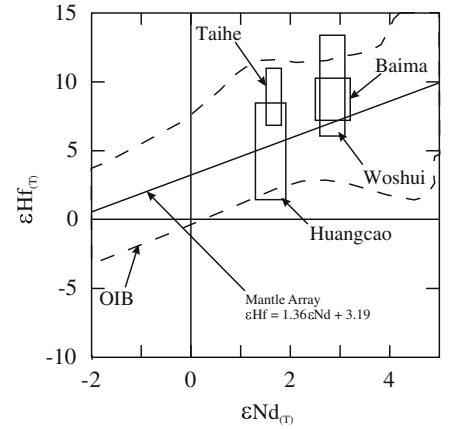

Fig. 4. $\varepsilon Nd_{(T)}$ vs. $\varepsilon Hf_{(T)}$ of the Hongge intrusion and the Baima, Taihe, Huangcao, and Woshui plutons. The range of ocean-island basalts shown as dashed line and the mantle array is calculated based on $\varepsilon Hf = 1.36\varepsilon Nd + 3.19$ (Vervoort and Blichert-Toft, 1999; Kempton et al., 2000). $\varepsilon Nd_{(T)}$ data from Shellnutt and Zhou (2007, 2008).

and Salian plutons may be derived from a mixed source, it is not likely the case for the Taihe pluton. If a rock is derived from a mixed source, evidence such as negative primitive mantle normalized Nb–Ta anomalies, negative $\varepsilon Nd_{(T)}$ values and high Ta/Th ratios are expected. The Taihe pluton does not have negative primitive mantle normalized Nb–Ta anomalies, positive $\epsilon Nd_{(T)}$ (+1.5 to +1.9) and the Th/Ta ratios are low (Shellnutt and Zhou, 2007). Therefore we suggest that the Taihe pluton is not derived from a mixed source and it likely represents the residual magma after fractionation of Emeishan high-Ti basalt (c.f. Shellnutt et al., in press). The two metaluminous (i.e. Woshui and Huangcao) plutons on the other hand are thought to be derived by partial melting of underplated mafic magmas and therefore could be considered as derived from juvenile crust (i.e. underplated Emeishan mafic magmas) however they are inherently products of ELIP magmatism and do not show evidence for crustal assimilation.

It should be noted that the Huangcao syenites (HC-2) as described by Xu et al. (2008) are not the same as the rocks from the Huangcao pluton initially described by Shellnutt and Zhou (2006) although the same name was applied. There are many differences between the two 'Huangcao' rocks. The samples described in detail by Shellnutt and Zhou (2008) are fayalite + quartz-bearing, ~252 Ma, have positive Eu/Eu∗ values (Eu/Eu∗ = 0.9–2.1), positive $\varepsilon Nd_{(T)}$ values ($\varepsilon Nd_{(T)}$ = +1.3 to +1.9) and have $\varepsilon Hf_{(T)} = +5.8 \pm 0.3$. The samples described by Xu et al. (2008) do not contain fayalite, are ~260 Ma, in a different location and have variable $\varepsilon Hf_{(T)}$.

4.2. Implications for the 252 Ma magmatism in the ELIP

There is a bimodal distribution of ages amongst the intrusive rocks of the Panxi region at ~260 and ~252 Ma with a minor group at ~240 Ma (Shellnutt et al., 2008; Xu et al., 2008) (Fig. 6). The peralkaline plutons and most of the metaluminous plutons have been dated at ~260 Ma (e.g. Baima, Taihe, Cida, Woshui, Maomaogou and Miyi) (Shellnutt and Zhou, 2007; Zhong et al., 2007; Xu et al., 2008; Shellnutt et al., in press). The Huangcao (metaluminous) and Ailanghe (peraluminous) plutons have been dated at ~252 Ma but have distinctly different origins. The Ailanghe pluton originated by melting of Yangtze Block basement rocks ($\varepsilon Nd_{(T)} = -5.7$ to -6.7; $\varepsilon Hf_{(T)} = -1.3$ to -4.4) whereas the Huangcao pluton was derived by partial melting of underplated Emeishan mafic rocks (Xu et al., 2008; Shellnutt and Zhou, 2007, 2008; Zhong et al., 2007). The magmatic event at ~252 Ma is thought to be related to either continuous Emeishan plume activity or to passive extension associated with the collision of the South China Block (i.e. Yangtze Block + Cathaysia Block) and Indochina Block (Shellnutt et al., 2008; Xu et al., 2008). It is unlikely that the 252 Ma magmatic event was a continuation of the 260 Ma magmatism because the Emeishan flood basalts erupted during one normal magnetic polarity episode and the terminal stage of ELIP magmatism is dated at 257 Ma and thus the heat source likely dissipated at the same time (Ali et al., 2005; He et al., 2007). Therefore, melting at 252 Ma likely occurred due to extension in the South China Block just prior to collision with the Indochina Block. We suggest that slab roll back may be the mechanism which triggered extension in the South China Block and induced melting of the underplated Emeishan material and the lower to middle crust which led to the formation of the Huangcao and Ailanghe plutons (Shellnutt et al., 2008).

4.3. Implications for metaluminous A-type granitic rocks

Peralkaline and metaluminous plutonic complexes are common within the continental crust (Poitrasson et al., 1995; Schmitt et al., 2000; Kemp et al., 2005). Metaluminous A-type granitic rocks are thought to be derived from a mixture of mantle and crustal components whereas peralkaline A-type granitic rocks are less likely to have a crustal component (Schmitt et al., 2000; Kemp et al., 2005; Bonin, 2007). Currently, there are few contemporaneous peralkaline–metaluminous plutonic complexes which report zircon Hf isotopic data however the Narraburra complex and Barmedman granite from Australia show a similar range of zircon Hf compositions as the granitic plutons of Panxi region (Fig. 7). The peralkaline Narraburra granites formed by fractionation of mantle-derived magmas whereas the metaluminous Barmedman granites formed by mixing of crustal rocks and juvenile magmas (Wormald et al., 2004; Kemp et al., 2005). The peralkaline plutons of the Panxi region and Narraburra likely formed by a similar process (i.e. fractionation of mantle-derived mafic magmas) and thus have similar zircon $\varepsilon H_{(T)}$ values. The metaluminous Barmedman granite and Huangcao pluton have a similar range of zircon $\varepsilon H_{(T)}$ whereas the Woshui pluton has $\varepsilon H_{(T)}$ values similar to the peralkaline plutons (Fig. 7). There is little evidence for crustal assimilation in the Woshui or Huangcao pluton which is contrasted with the mixed crust + juvenile magma origin of the Barmedman granite. The Ba/Nb, Rb/Nb and Nb/Y ratios of the Barmedman (Ba/Nb = 24.8; Rb/Nb = 9.9; Nb/Y = 0.3) are closer to average continental crust

(upper crust, Ba/Nb = 25.7; Rb/Nb = 4.2; Nb/Y = 1.3; lower crust, Ba/Nb = 50.3; Rb/Nb = 3.6; Nb/Y = 0.4) and considerably different from the Woshui (Ba/Nb = 27.9; Rb/Nb = 1.2; Nb/Y = 1.4) and Huangcao plutons (Ba/Nb = 43.7; Rb/Nb = 2.6; Nb/Y = 1.5), attesting to their differing origins (Wedepohl, 1995; Wormald et al., 2004). The implication is that the metaluminous plutons (i.e. Woshui and Huangcao) may originate from the same source as their peralkaline counterparts (i.e. Baima and Taihe) without any significant contribution from the crust.

An important difference between the plutons of the Panxi region and the Narraburra–Barmedman suites is their tectonomagmatic setting. The Narraburra–Barmedman suites were formed by lithospheric extension which exploited crustal-scale faults related to previously thinned crust during slab roll back (Wormald et al., 2004; Kemp et al., 2005). Thus the Narraburra–Barmedman suites were produced by melting of lithospheric mantle and assimilation of crustal material at various proportions giving rise to a mixed zircon Hf signature. In contrast the metaluminous and peralkaline plutons of the Panxi region were formed within an intraplate extensional setting associated with a mantle plume (Xu et al., 2004; He et al., 2007; Shellnutt and Zhou, 2007). The parental magmas of the plutons in the Panxi region likely formed at depths

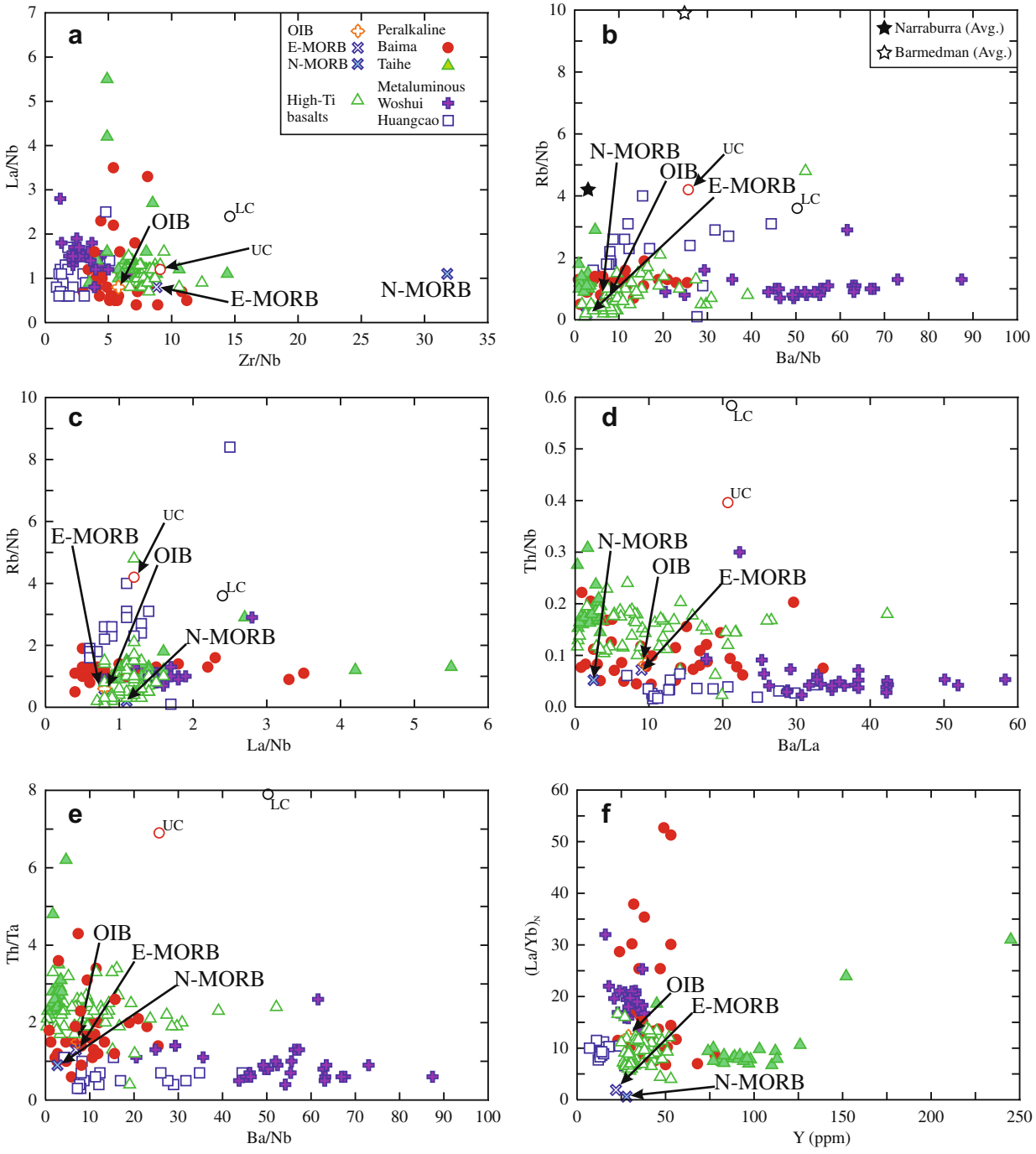

Fig. 5. Trace element ratio comparison of the Panxi A-type granitoids with the Emeishan flood basalt, upper crust, lower crust, OIB, N-MORB and E-MORB. Emeishan data from Xu et al. (2001), Xiao et al. (2004), Wang et al. (2007) and Shellnutt and Zhou (2007, 2008). UC, upper crust; LC, lower crust (Wedepohl, 1995). N-MORB, normal mid-ocean ridge basalt; E-MORB, enriched mid-ocean ridge basalt; OIB, ocean-island basalt data from Sun and McDonough (1989). Data for the Narraburra and Barmedman granitic rocks from Wormald et al. (2004).

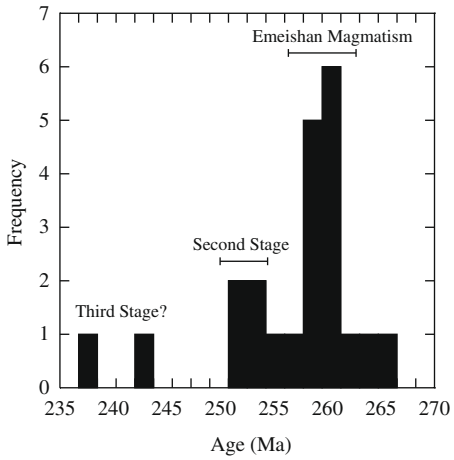

Fig. 6. Distribution of published U–Pb dates from the ELIP. Data from Zhou et al. (2002, 2005, 2006), Fan et al. (2004), Guo et al. (2004), Zhong and Zhu (2006), He et al. (2007), Zhong et al. (2007, 2009), Shellnutt and Zhou (2007, 2008), Shellnutt et al. (in press) and Xu et al. (2008). One result is currently unpublished.

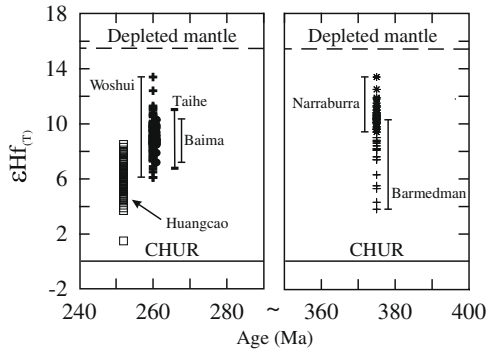

Fig. 7. $\varepsilon Hf_{(T)}$ vs. age of the Panxi plutons and Narraburra and Barmedman suites from Kemp et al. (2005). The data fall between depleted mantle and the chondrite uniform reservoir (CHUR).

of ~200 to 400 km by low degrees of partial melting of enriched mantle material (Wang et al., 2007). The high-Ti basaltic magmas were probably volatile-rich, as evidenced by the presence of primary biotite in these rocks (Xu et al., 2001). The relatively light and volatile-rich high-Ti magmas could have ascended rapidly to the surface, such that they escaped crustal contamination.

5. Conclusion

Zircon Hf isotopic values of the Baima, Taihe, Woshui and Huangcao plutons are indicative of their mantle source. Trace element data are consistent with previous interpretations of the enriched mantle source for the high-Ti Emeishan basaltic rocks and show that there is little, if any crustal contamination in the plutons. The important implication of the results is that spatially and temporally associated peralkaline and metaluminous plutons (e.g. Baima and Taihe) can originate by different processes from the same mantle source without crustal assimilation.

Acknowledgements

We acknowledge the constructive reviews by Jin-Hui Yang and Sun-Lin Chung and the editorial handling by Bor-Ming Jahn. The authors would like to thank Dr. Liang Qi and Ms. Xiao Fu for their analytical support at the University of Hong Kong. This study is supported by Academia Sinica, Institute of Earth Sciences and grants from the Research Grant Council of Hong Kong, SAR (HKU7065/06P) and Chinese 973 Project (2007CB411401).

References

Ali, J.R., Thompson, G.M., Zhou, M.-F., Song, X.Y., 2005. Emeishan large igneous province, SW China. Lithos 79, 475–489.
Blichert-Toft, J., Frey, F.A., Albarede, F., 1999. Hf isotope evidence for pelagic sediments in the source of Hawaiian basalts. Science 285, 879–882.
Bonin, B., 2007. A-type granites and related rocks: evolution of a concept, problems and prospects. Lithos 97, 1–29.
Chauvel, C., Blichert-Toft, J., 2001. A hafnium and trace element perspective on melting of the depleted mantle. Earth and Planetary Science Letters 190, 137–151.
Chauvel, C., Lewin, E., Carpenter, M., Arndt, N.T., Marini, J.-C., 2008. Role of the recycled oceanic basalt and sediment in generating the Hf–Nd mantle array. Nature Geoscience 1, 64–67.
Chu, N.C., Taylor, R.N., Chavagnac, V., Nesbitt, R.W., Boella, R.M., Milton, J.A., German, C.R., Bayon, G., Burton, K., 2002. Hf isotope ratio analysis using multi-collector inductively coupled plasma mass spectrometry: an evaluation of isobaric interference corrections. Journal of Analytical Atomic Spectrometry 17, 1567–1574.
Chung, S.L., Jahn, B.-M., 1995. Plume–lithosphere interaction in generation of the Emeishan flood basalts at the Permian–Triassic boundary. Geology 23, 889–892.
Chung, S.L., Jahn, B.M., Genyao, W., Lo, C.H., Bolin, C., 1998. The Emeishan flood basalts in SW China: a mantle plume initiation model and its connection with continental breakup and mass extinction at the Permian–Triassic boundary. In: Flower, M.F.J., Chung, S.-L., Lo, C.-H., Lee, T.-Y (Eds.), Mantle Dynamics and Plate Interactions in East Asia, American Geophysical Union Geodynamic Series, vol. 27, pp. 47–58.
Collins, W.J., Beams, S.D., White, A.J.R., Chappell, B.W., 1982. Nature and origin of A-type granites with particular reference to southeastern Australia. Contributions to Mineralogy and Petrology 80, 189–200.
Eby, G.N., 1992. Chemical subdivisions of the A-type granitoids: petrogenetic and tectonic implications. Geology 20, 641–644.
Fan, W., Wang, V., Peng, T., Miao, L., Guo, F., 2004. Ar–Ar and U–Pb geochronology of late Paleozoic basalts in western Guangxi and its constraints on the eruption age of Emeishan basalt magmatism. Chinese Science Bulletin 49, 2318–2327.
Frost, C.D., Frost, B.R., 1997. Reduced rapakivi-type granites: the tholeiite connection. Geology 25, 647–650.
Goodge, J.W., Vervoort, J.D., 2006. Origin of Mesoproterozoic A-type granites in Laurentia: Hf isotope evidence. Earth and Planetary Science Letters 243, 711–731.
Griffin, W.L., Belousova, E.A., Walters, S.G., O'Reilly, S.Y., 2006. Archaean and Proterozoic crustal evolution in the eastern succession of the Mt Isa district, Australia: U–Pb and Hf-isotope studies of detrital zircons. Australian Journal of Earth Sciences 53, 125–149.
Griffin, W.L., Pearson, N.J., Belousova, E., Jackson, S.E., van Achterbergh, E., O'Reilly, S.Y., Shee, S.R., 2000. The Hf isotope composition of cratonic mantle: LAM-MC-ICPMS analysis of zircon megacrysts in kimberlites. Geochimica et Cosmochimica Acta 64, 133–147.
Guo, F., Fan, W., Wang, Y., Li, C., 2004. When did the Emeishan mantle plume activity start? Geochronological and geochemical evidence from ultramafic–mafic dikes in southwestern China. International Geology Review 46, 226–234.
He, B., Xu, Y.-G., Huang, X.-L., Luo, Z.-Y., Shi, Y.-R., Yang, O.-J., Yu, S.-Y., 2007. Age and duration of the Emeishan flood volcanism, SW China: geochemistry and SHRIMP zircon U–Pb dating of silicic ignimbrites, post-volcanic Xuanwei Formation and clay tuff at the Chaotian section. Earth and Planetary Science Letters 255, 306–323.
Kemp, A.I.S., Hawkesworth, C.J., Foster, G.L., Paterson, B.A., Woodhead, J.D., Hergt, J.M., Gray, C.M., Whitehouse, M.J., 2007. Magmatic and crustal differentiation history of granitic rocks from Hf–O isotopes in zircon. Science 315, 980–983.
Kemp, A.I.S., Wormald, R.J., Whitehouse, M.J., Price, R.C., 2005. Hf isotopes in zircon reveal contrasting sources and crystallization histories for alkaline to peralkaline granites of Temora, southeastern Australia. Geology 33, 797–800.
Kempton, P.D., Fitton, J.G., Saunders, A.D., Nowell, G.M., Taylor, R.N., Hardarson, B.S., Pearson, G., 2000. The Iceland plume in space and time: a Sr–Nd–Pb–Hf study of the North Atlantic rifted margin. Earth and Planetary Science Letters 177, 255–271.
King, P.L., White, A.J.R., Chappell, B.W., Allen, C.M., 1997. Characterization and origin of aluminous A-type granites from the Lachlan fold belt, southeastern Australia. Journal of Petrology 38, 371–391.
Kinny, P.D., Maas, R., 2003. Lu–Hf and Sm–Nd isotope systems in zircon. In: Hanchar, J.M., Hoskin, P.W.O. (Eds.), Zircon. Reviews in Mineralogy and Geochemistry 53, 327–341.
Loiselle, M.C., Wones, D.R., 1979. Characteristics and origin of anorogenic granites. Geological Society of America Abstract with Programs 11, 468.
Machado, N., Simonetti, A., 2001. U–Pb dating and Hf isotopic composition of zircons by laser ablation–MC–ICP–MSA. In: Sylvester, P. (Ed.), Laser Ablation ICPMS in the Earth Sciences: Principles and Applications, Short Course, Mineralogical Association of Canada, vol. 29, pp. 121–146.
Nowell, G.M., Kempton, P.D., Noble, S.R., Fitton, J.G., Saunders, A.D., Mahoney, J.J., Taylor, R.N., 1998. High precision Hf isotopic measurements of MORB and OIB by thermal ionization mass spectrometry: insights into the depleted mantle. Chemical Geology 149, 211–233.

Patchett, P.J., Tatsumoto, M., 1980. Hafnium isotope variations in oceanic basalts. Geophysical Research Letters 7, 1077–1080.
Poitrasson, F., Paquette, J.L., Montel, J.M., Pin, C., Duthou, J.L., 1998. Importance of late-magmatic and hydrothermal fluids on the Sm–Nd isotope mineral, systematics of hypersolvus granites. Chemical Geology 146, 187–203.
Poitrasson, F., Duthou, J.-L., Pin, C., 1995. The relationship between petrology and Nd isotopes as evidence for contrasting anorogenic granite genesis: example of the Corsican Province. Journal of Petrology 36, 1251–1274.
Salters, V.J.M., 1996. The generation of mid-ocean ridge basalts from the Hf and Nd isotope perspective. Earth and Planetary Science Letters 141, 109–123.
Salters, V.J.M., White, W.M., 1998. Hf isotope constraints on mantle evolution. Chemical Geology 145, 447–460.
Schmitt, A.K., Emmermann, R., Trumbull, R.B., Buhn, B., Henjes-Kunst, F., 2000. Petrogenesis and $^{40}Ar/^{39}Ar$ geochronology of the Brandberg Complex, Namibia: evidence for a major mantle contribution in metaluminous and peralkaline granites. Journal of Petrology 41, 1207–1239.
Shellnutt, J.G., Zhou, M.-F., Zellmer, G., in press. The role of Fe–Ti oxide crystallization in the formation of A-type granitoids with implications for the Daly gap: an example from the Permian Baima Igneous Complex. Chemical Geology. doi:10.1016/j.chemgeo.2008.10.044.
Shellnutt, J.G., Zhou, M.-F., Yan, D.-P., Wang, Y., 2008. Longevity of the Permian Emeishan mantle plume (SW China): 1 Ma, 8 Ma or 18 Ma? Geological Magazine 145, 373–388.
Shellnutt, J.G., Zhou, M.-F., 2008. Rifting-related, Permian fayalite syenite in the Panxi region, SW China. Lithos 101, 54–73.
Shellnutt, J.G., Zhou, M.-F., 2007. Permian peralkaline, peraluminous and metaluminous A-type granites in the Panxi district, SW China: their relationship to the Emeishan mantle plume. Chemical Geology 243, 286–316.
Shellnutt, J.G., Zhou, M-F., 2006. Rifting-related, Permian ferrosyenites in the Panxi region of the Emeishan large igneous province, SW China. Geochimica et Cosmochimica Acta 70, 579.
Song, X.-Y., Qi, H.-W., Robinson, P.T., Zhou, M.-F., Cao, Z.-M., Chen, L.-M., 2008. Melting of the subcontinental lithospheric mantle by the Emeishan mantle plume; evidence from the basal alkaline basalts in Dongchuan, Yunnan, Southwestern China. Lithos 100, 93–111.
Sun, S.S., McDonough, W.F., 1989. Chemical and isotopic systematics of oceanic basalts: implications for mantle composition and processes. In: Saunders, A.D., Norry, M.J. (Eds.), Magmatism in the Ocean Basins. Geological Society of London Special Publication 42, 313–435.
Turner, S.P., Foden, J.D., Morrison, R.S., 1992. Derivation of some A-type magmas by fractionation of basaltic magma: an example from the Padthaway Ridge, south Australia. Lithos 28, 151–179.
Vervoort, J.D., Blichert-Toft, J., 1999. Evolution of the depleted mantle: Hf isotope evidence from juvenile rocks through time. Geochimica et Cosmochimica Acta 63, 533–556.
Vervoort, J.D., Patchett, P.J., Gehrels, G.E., Nutman, A.P., 1996. Constraints on early Earth differentiation from hafnium and neodymium. Nature 379, 624–627.
Wang, C.Y., Zhou, M.-F., Qi, L., 2007. Permian flood basalts and mafic intrusions in the Jinping (SW China)–Song Da (northern Vietnam) district: mantle sources, crustal contamination and sulfide segregation. Chemical Geology 243, 317–343.
Weaver, B.L., 1991. The origin of ocean island basalt end-member compositions: trace element and isotopic constraints. Earth and Planetary Science Letters 104, 381–397.
Wedepohl, K.H., 1995. The composition of the continental crust. Geochimica et Cosmochimica Acta 59, 1217–1232.
Whalen, J.B., Currie, K.L., Chappell, B.W., 1987. A-type granites: geochemical characteristics, discrimination and petrogenesis. Contributions to Mineralogy and Petrology 95, 407–419.
Woodhead, J., Hergt, J., Shelley, M., Eggins, S., Kemp, R., 2004. Zircon Hf-isotope analysis with an excimer laser, depth profiling, ablation of complex geometries, and concomitant age estimation. Chemical Geology 209, 121–135.
Wormald, R.J., Price, R.C., Kemp, A.I.S., 2004. Geochemistry and Rb–Sr geochronology of the alkaline–peralkaline Narraburra Complex, central southern New South Wales; tectonic significance of the Late Devonian granitic magmatism in the Lachlan fold belt. Australian Journal of Earth Sciences 51, 369–384.
Wu, F.-Y., Yang, Y.-H., Xie, L.-W., Yang, J.-H., Xu, P., 2006. Hf isotopic compositions of the standard zircons and baddeleyites used in U–Pb geochronology. Chemical Geology 234, 105–126.
Wu, F.-Y., Sun, D.-Y., Li, H., Jahn, B.-M., Wilde, S., 2002. A-type granites in northeastern China: age and geochemical constraints on their petrogenesis. Chemical Geology 187, 143–173.
Xiao, L., Xu, Y.G., Mei, H.J., Zheng, Y.F., He, B., Pirajno, F., 2004. Distinct mantle sources of low-Ti and high-Ti basalts from the western Emeishan large igneous province, SW China: implications for plume–lithosphere interaction. Earth and Planetary Science Letters 228, 525–546.
Xu, Y.-G., Luo, Z.-Y., Huang, X.-L., He, B., Xiao, Xie, L.-W., Shi, Y.-R., 2008. Zircon U–Pb and Hf isotope constraints on crustal melting associated with the Emeishan mantle plume. Geochimica et Cosmochimica Acta 72, 3084–3104.
Xu, Y.G., He, B., Chung, S.L., Menzies, M., Frey, F.A., 2004. Geologic, geochemical, and geophysical consequences of plume involvement in the Emeishan flood-basalt province. Geology 32, 917–920.
Xu, Y.G., Chung, S.L., Jahn, B.-M., Wu, G., 2001. Petrologic and geochemical constraints on the petrogenesis of Permian–Triassic Emeishan flood basalts in southwestern China. Lithos 58, 145–168.
Yang, J.-H., Wu, F.-Y., Chung, S.-L., Wilde, S.A., Chu, M.-F., 2006. A hybrid origin for the Qianshan A-type granite, northeast China: geochemical and Sr–Nd–Hf isotopic evidence. Lithos 89, 89–106.
Zhong, H., Zhu, W.-G., Song, X.-Y., He, D.-F., 2007. SHRIMP U–Pb zircon geochronology, geochemistry, and Nd–Sr isotopic study of contrasting granites in the Emeishan large igneous province, SW China. Chemical Geology 236, 112–133.
Zhong, H., Zhu, W.G., 2006. Geochronology of layered mafic intrusions from the Pan-Xi area in the Emeishan large igneous province, SW China. Mineralium Deposita 41, 599–606.
Zhong, H., Hu, R.-Z., Wilson, A.H., Zhu, W.-D., 2005. Review of the link between the Hongge layered intrusion and Emeishan Flood Basalts, Southwest China. International Geology Review 47, 971–985.
Zhong, H., Zhu, W.-G., Hu, R.-Z., Xie, L.-W., He, D.-F., Liu, F., Chu, Z.-Y., 2009. Zircon U–Pb age and Sr–Nd–Hf isotope geochemistry of the Panzhihua A-type syenitic intrusion in the Emeishan large igneous provience, southwest China and implications for growth of juvenile crust. Lithos, in press, doi:10.1016/j.lithos.2008.12.006.
Zhou, M.-F., Arndt, N.T., Malpas, J., Wang, C.Y., Kennedy, A.K., 2008. Two magma series and associated ore deposit types in the Permian Emeishan large igneous province, SW China. Lithos 103, 352–368.
Zhou, M.-F., Zhao, J.H., Qi, L., Su, W., Hu, R.Z., 2006. Zircon U–Pb geochronology and elemental and Sr–Nd isotopic geochemistry of Permian mafic rocks in the Funing area, SW China. Contributions to Mineralogy and Petrology 151, 1–19.
Zhou, M.-F., Robinson, P.T., Lesher, C.M., Keays, R.R., Zhang, C.J., Malpas, J., 2005. Geochemistry, petrogenesis and metallogenesis of the Panzhihua gabbroic layered intrusion and associated Fe–Ti–V oxide deposits, Sichuan Province, SW China. Journal of Petrology 46, 2253–2280.
Zhou, M.-F., Malpas, J., Song, X.-Y., Robinson, P.T., Sun, M., Kennedy, A.K., Lesher, C.M., Keays, R.R., 2002. A temporal link between the Emeishan large igneous province (SW China) and the end-Guadalupian mass extinction. Earth and Planetary Science Letters 196, 113–122.